A deep resistivity Full Waver survey unravels the 3D structure of the Castelluccio basin in relation to the source of the 2016 Mw 6.5 Norcia earthquake (central Italy)

Vincenzo Sapia[1], *Fabio Villani*[1], *Federico Fischanger*[2], *Matteo Lupi*[3], *Paola Baccheschi*[1], *Carlo Alberto Brunori*[1], *Riccardo Civico*[1], *Igino Coco*[1], *Paolo Marco De Martini*[1], *Fabio Giannattasio*[1], *Luigi Improta*[1], *Valerio Materni*[1], *Federica Murgia*[4], *Daniela Pantosti*[1], *Luca Pizzimenti*[1], *Stefano Pucci*[1], *Tullio Ricci*[1], *Valentina Romano*[4], *Alessandra Sciarra*[1], *Alessandra Smedile*

*1 Istituto Nazionale di Geofisica e Vulcanologia, Rome, Italy (**vincenzo.sapia@ingv.it**)*
2 Geostudi Astier srl
3 Universitè de Geneve
4 Università degli Studi di Roma La Sapienza

Geological and Seismotectonic Background

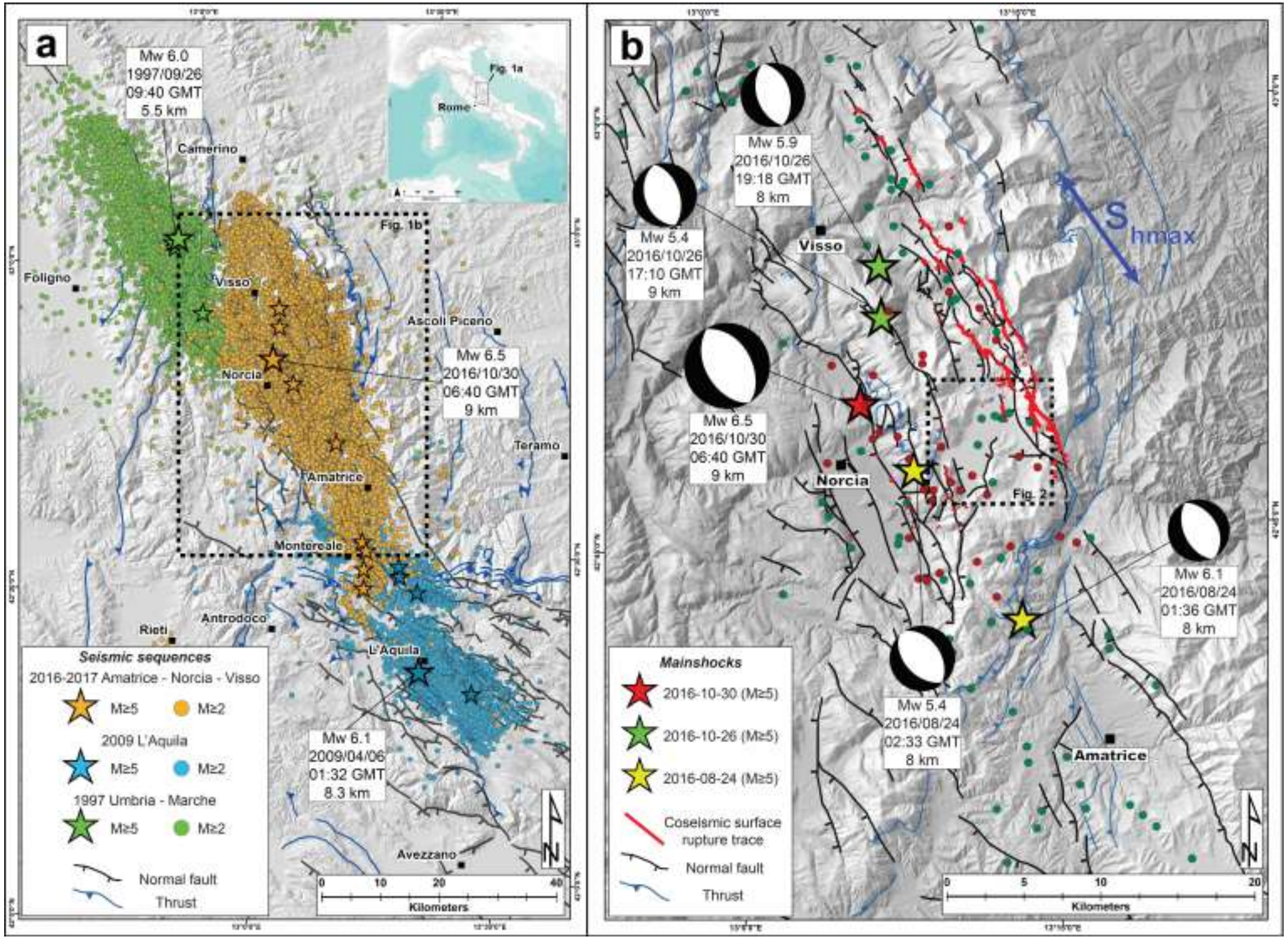

The seismic sequence that hits the central Italy in 2016-2017 was caused by the activation of the ~25 km-long Mt. Vettore - Mt. Bove (VBFS) and the Laga Mts. fault-systems (LMFS), culminating with the 30 October 2016 earthquake near Norcia (Mw 6.5). The Pian Grande Castelluccio basin (PGC) is an intramontane Quaternary depression, bounded by differently oriented faults: in particular, the Mt. Vettore normal faults to the NE ruptured the surface during the Norcia earthquake on several splays.

a) Quaternary normal faults (black lines), principal thrusts (blue lines) and the three main seismic sequences occurring since 1997 (the stars indicate events with M>5). b) Sibillini Mts. area, showing the trace of the coseismic surface ruptures following the 30 October 2016 Mw 6.5 Norcia earthquake (modifed after Civico et al., 2018) and focal mechanisms of the mainshocks of the Amatrice-Visso-Norcia sequence.

From Villani and Sapia 2017 , Tectonophysics

A

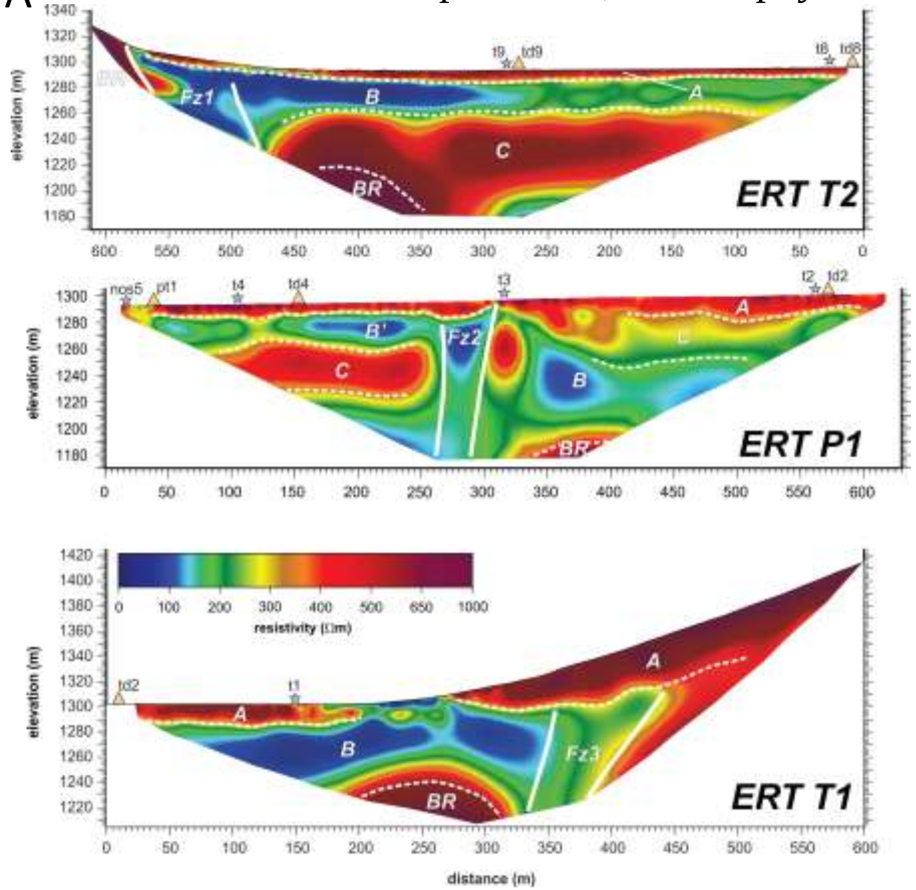

Previous Geophysical Results

Previous geophysical results over the PGC basin, highlighted an asymmetric graben structure up to 300 m deep and consisting of several splays with different degree of activity. The overall setting is related to the interference pattern of two differently orientated fault systems: 1) an older, N30°-striking system; 2) a younger and still active N150° striking system.

B

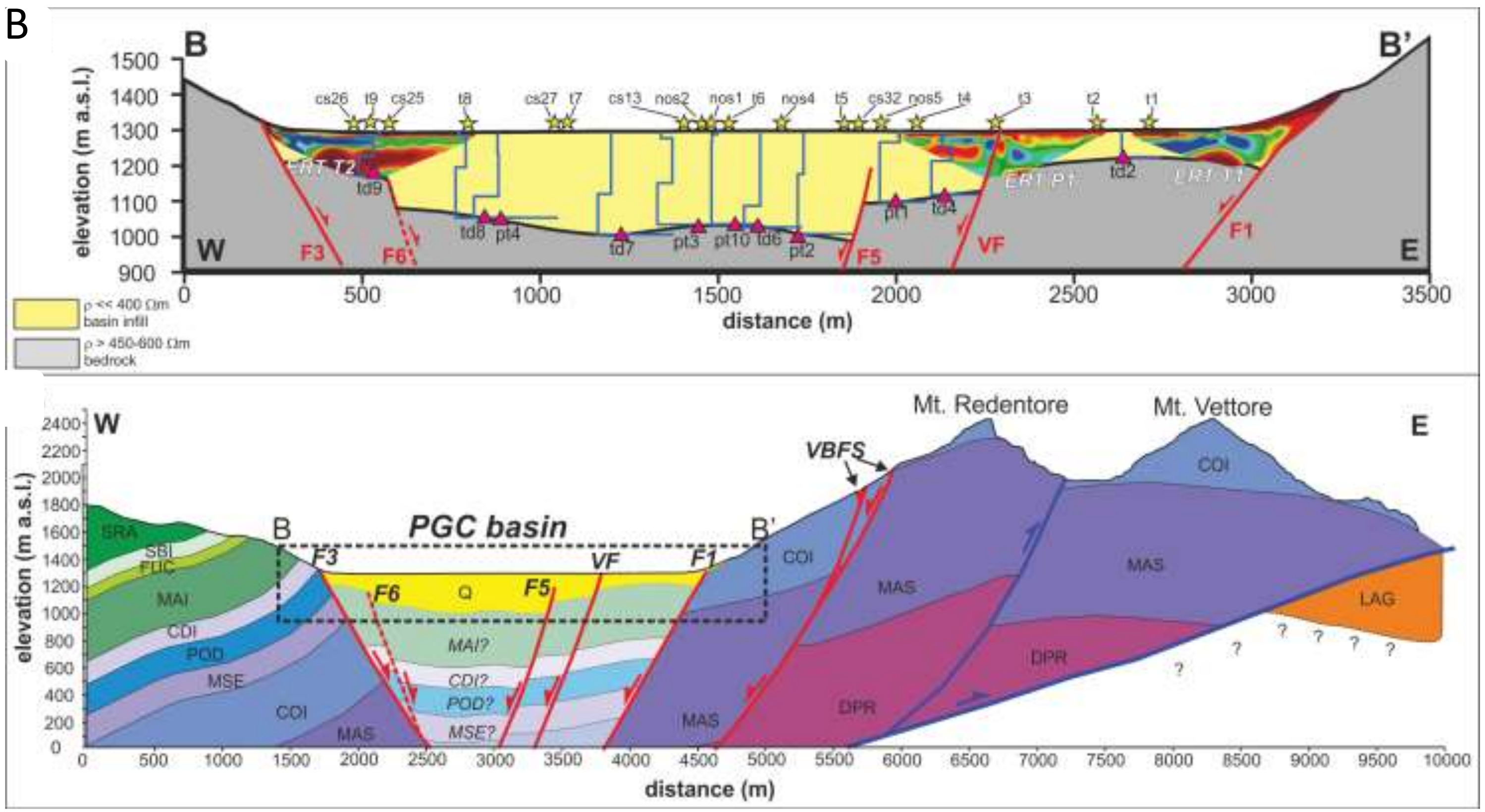

*A - The dashed lines indicate approximate boundaries of the main electrical units: A and C: alluvial fan deposits; B: fluvio-lacustrine deposits; BR: carbonate bedrock. The lateral extent of the inferred fault zones (**units Fz**) is shown with solid white lines.*

B - Interpretative geological cross-section across the PGC basin by combining geophysical and geological data. The label formations are; LAG is Miocene flysch; Q is the generic Quaternary continental infill). VBFS indicates the uppermost splays (Cordone del Vettore fault) that ruptured during the Norcia earthquake. The inferred stratigraphy beneath the basin is coloured with transparency.

From Villani et al., 2019, Tectonics

Available boreholes and geophysical dataset are not enough to constrain the basin structure, infill architecture and their relations with the long term activity of the VBFS.

TO THIS END

We carried out an extensive 3D survey using the innovative Fullwaver (FW) technology, conceived to perform deep electrical resistivity tomography (DERT).

WE AIMED AT

a) mapping the 3D geometry of the pre-Quaternary limestone basement and the basin infill architecture down to a depth of ~1.5 km;

b) mapping the subsurface structure of known faults and their extent underneath the basin infill;

c) mapping possible blind faults splays over the entire PGC basin;

d) imaging the subsurface expression of the 2016 coseismic ruptures along a 2-D high-resolution transect

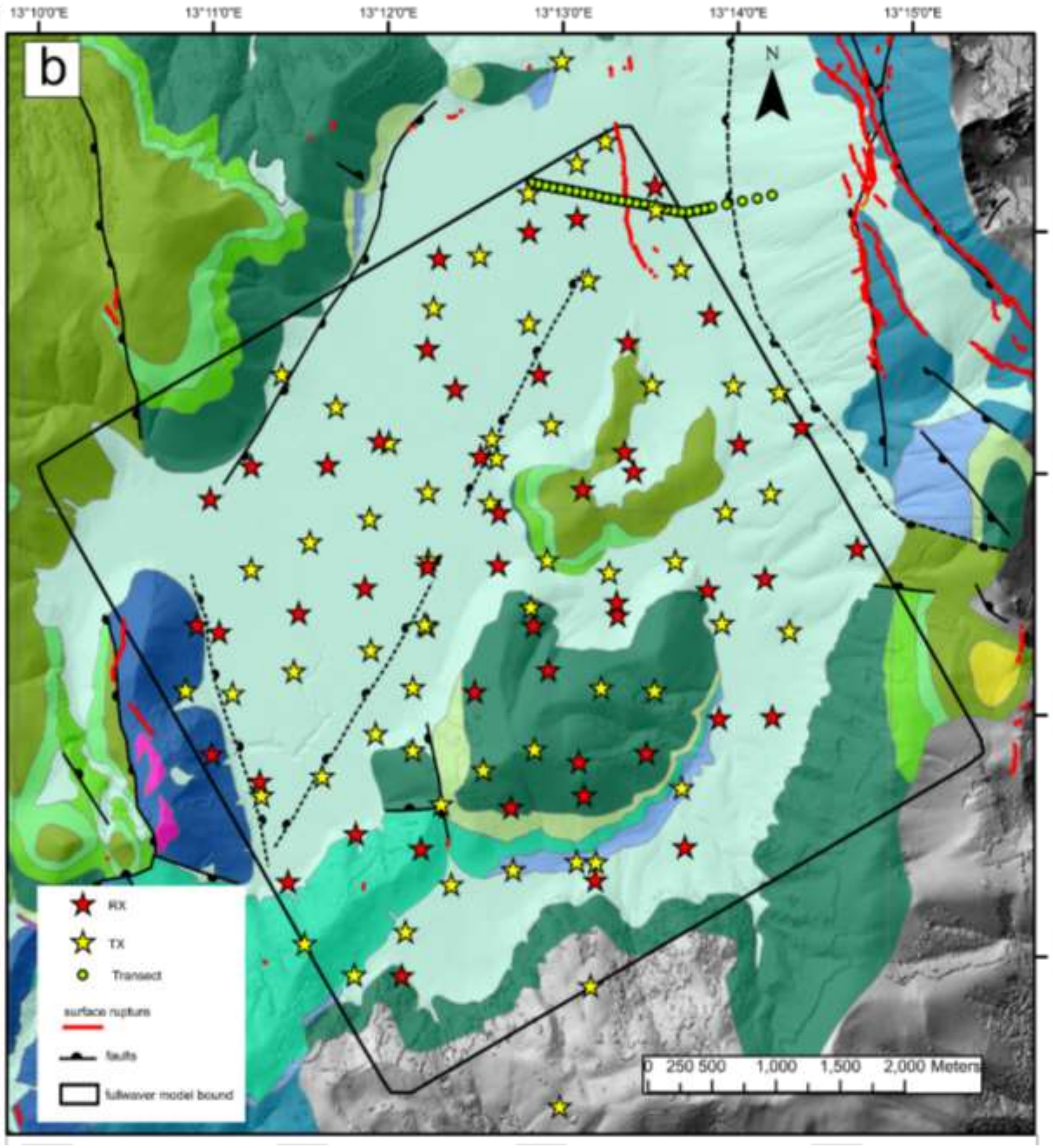

Method and survey design

Geological map of the PGC basin superimposed on the DEM showing the geophysical survey area (black box), the location of Fullwaver transmitters (yellow stars) and receiver (red stars) boxes and the trace of the 2D high resolution Fullwaver transect (T-T')

The 3D survey was designed with the aim to map the area as regularly as possible, taking into account the rough topography and the accessibility to the measurement sites. Due to a limited number of Fullwaver receiver boxes (24 Rx) and logistics, the area has been subdivided in two subset survey areas respectively the West and East. Each Fullwaver receiver boxes was connected to 3 steel electrodes deployed in a line. Dipole length was set to 200 m and was adjusted according to logistic (e.g. roads, field borders and topography). All trasmissions were aligned along almost parallel paths and set within the arranged Rx grid (24x2 Rx positions) for a total number of 50 Tx positions

The 2-D high-resolution transect that complements the 3-D survey targets a fault splay of the VBFS that ruptured during both the Mw 6.5 2016 mainshock and holocene paleoearthquakes (Galli & Galadini, 2003). The 2D resistivity profile, West – East oriented, is centered on the 30 October 2016 Mw 6.5 Earthquake surface rupture. The high resolution transect was measured deploying 24 RX boxes with roll along scheme in order to cover a profile length of 1.4 km using a constant spacing of 15 m between receiver and transmitter dipole electrodes

A

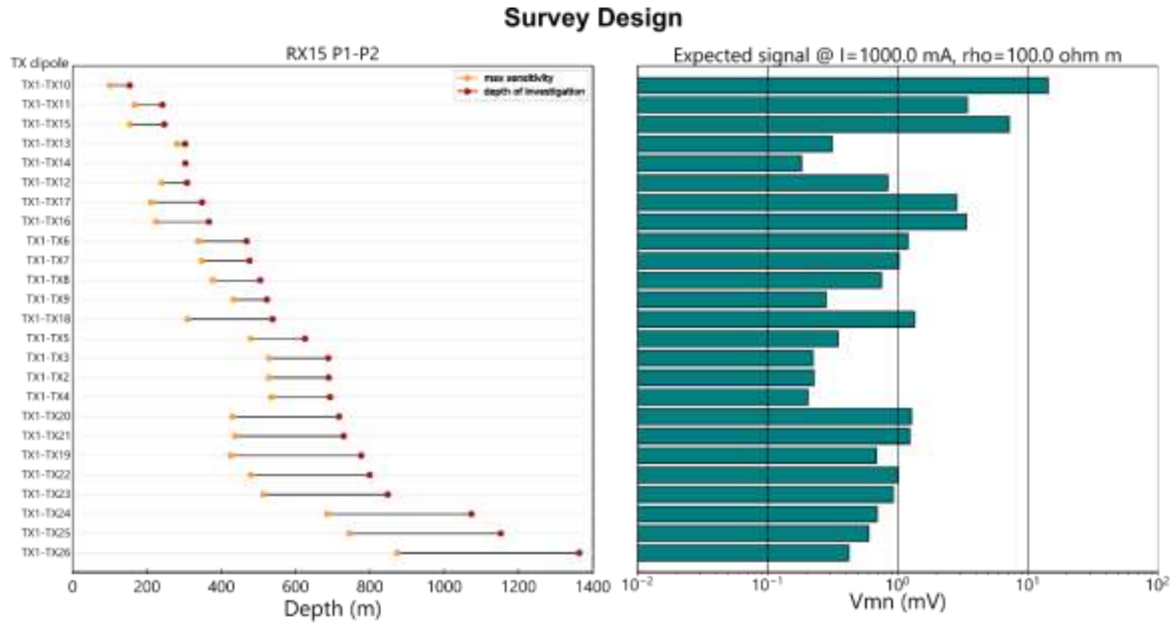

B

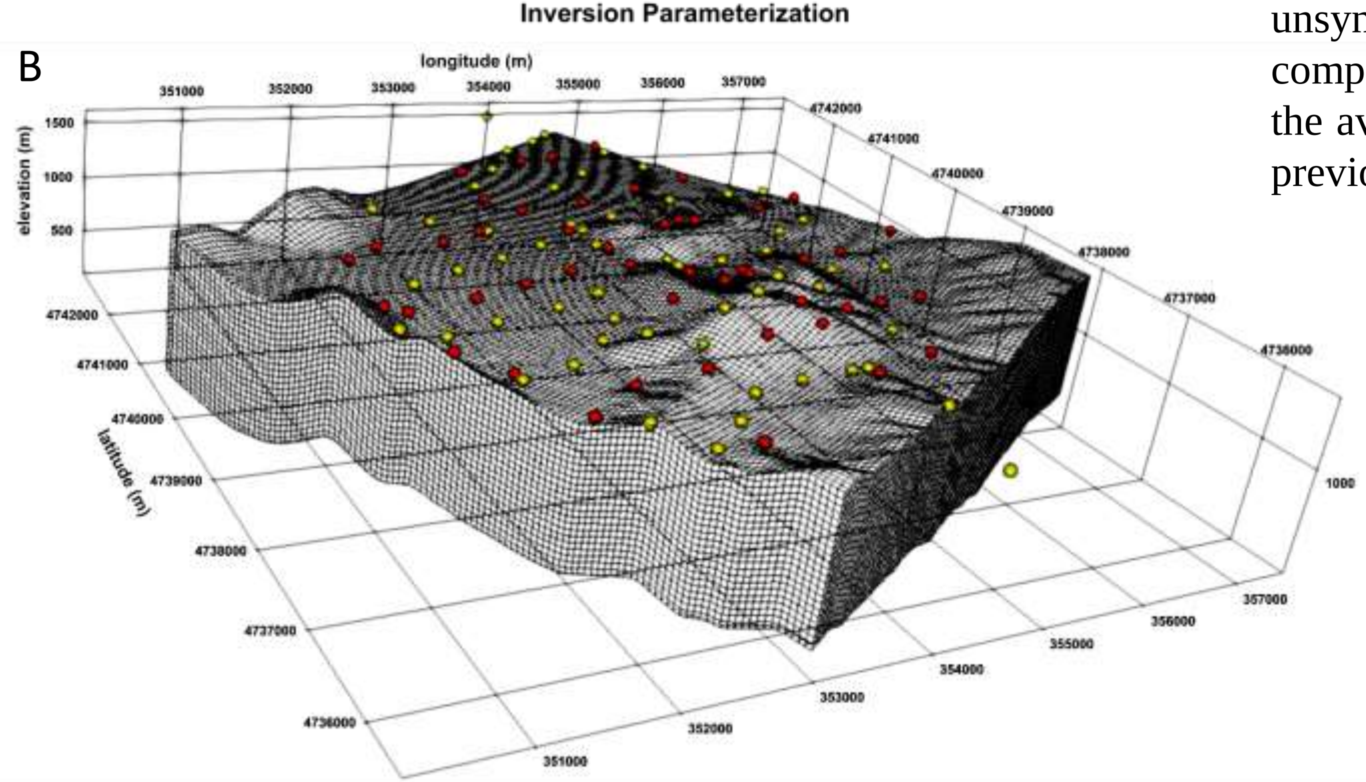

Method and survey design

Beside logistic, the design of the survey also consisted in verifying the level of signal at each receiver boxes for all transmissions down to a depth of about 1.5 km. As an example, we used a Dumbbell plot to graph the maximum sensitivity and the maximum depth of investigation expected for a receiver placed at the middle of the survey area for each transmitter positions (Fig. A left). We also show the expected signal to the same receiver in the hypothesis of a background resistivity of 100 Ohm.m and for an injected current of 1 Amp (Fig. A right).

Data processing consisted of re-synchronizing possibly unsynchronized time series, filtering spikes and self-potential jumps, computing of the average voltages on the stacked period, computing the average on the stacked period and calculating the resistance from previous measurements

We built a finite element 3D mesh with 50m x 50m x 50m cells size and 1200 m foreground depth (Fig. B). We parametrize the inversion using a starting model of 1000 Ohm.m and "**anisotropic**" roughness x = 1, y = 1, z = 0.01 to enhance resistivity variations in the z direction. Estimated noise on the data was set equal to 1% for V / I ratio. For the 2D transect we built a mesh with 5m x 5m x 5m cell size and 350 m foreground depth. We parametrize the inversion using a starting model of 500 Ohm.m and "**isotropic**" roughness x = 1, y = 1, z = 1. Estimated noise on the data was set equal to 0.5% for V / I ratio.

Results

Processed data were modeled with a regularized 3D inversion algorithm using smoothness constraints along x and y and sharp constraints along z direction in order to highlight strong resistivity changes expected in the interface between basin infill and the carbonate substratum

The first step of our model interpretation was to assign lithology to specific regions of the recovered electrical property models – **RESISTIVITY CLASSIFICATION**

This classification is guided by the experience gained after several geophysical surveys in the central Apennine. We learned that loose sediments with alternating coarse and fine elements show resistivity values ranging between 20 to 200 Ohm.m while marly limestones to massive carbonatic rocks exhibit higher resistivity ranging from ~700 to ≥ 2000 Ohm.m, respectively.

Top: frequency histogram of resistivity values from the full 3D model (logarithmic scale; bin size 10 Ωm); the vertical dashed lines indicate classification boundaries of the main electrical units defined in this work (red bars enclose modal peak around the starting 1000 Ωm background value, which mostly characterizes the model borders). **Bottom:** statistical parameters of resistivity vs. depth (minimum value, first interquartile, median, third interquartile) extracted from 24 layers spaced 50 m apart along z-direction; the blue polygon indicates the inferred contribution from the PGC basin infill material.

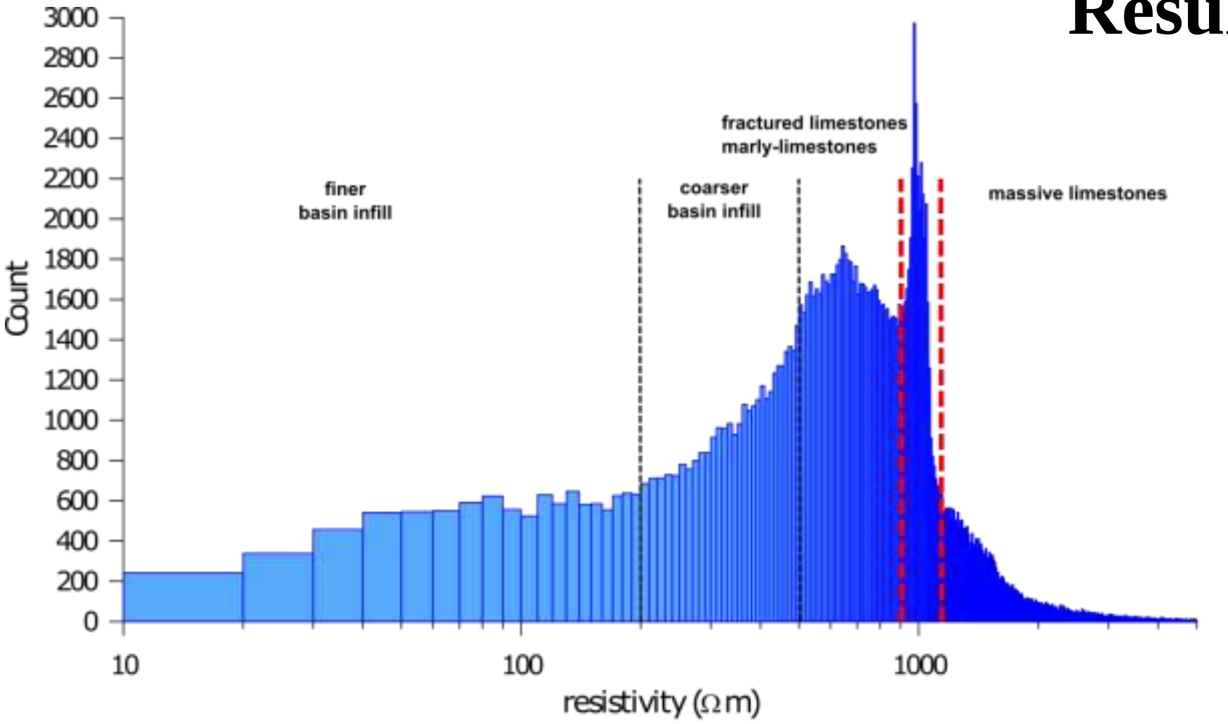

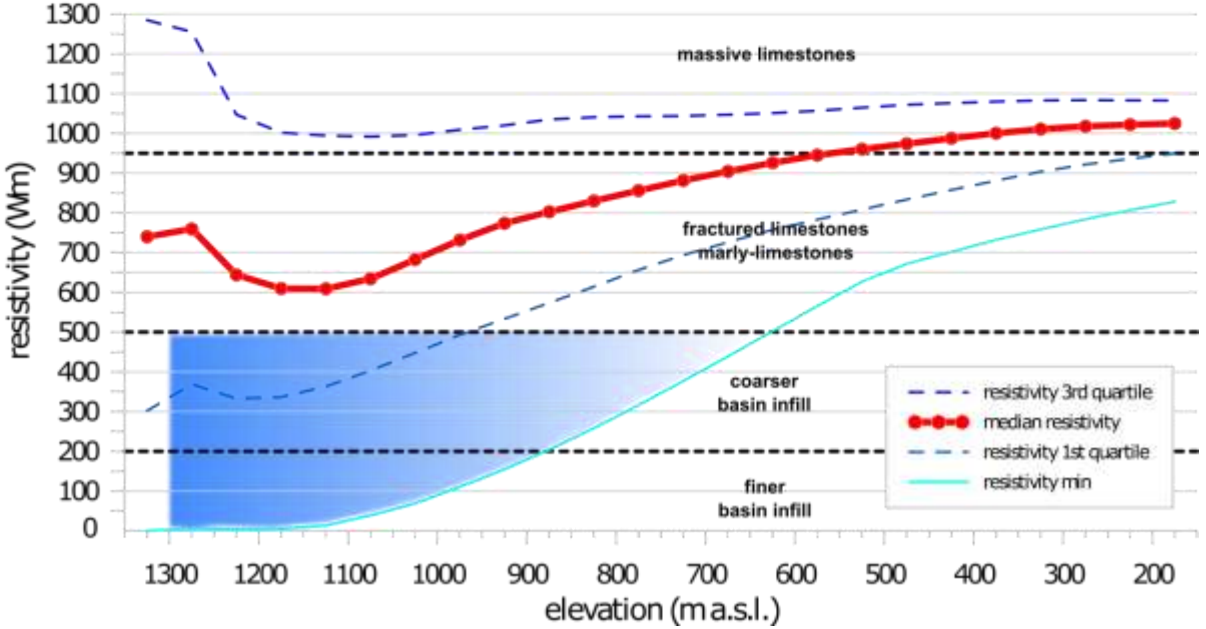

2-D high-resolution transect

RESULTS

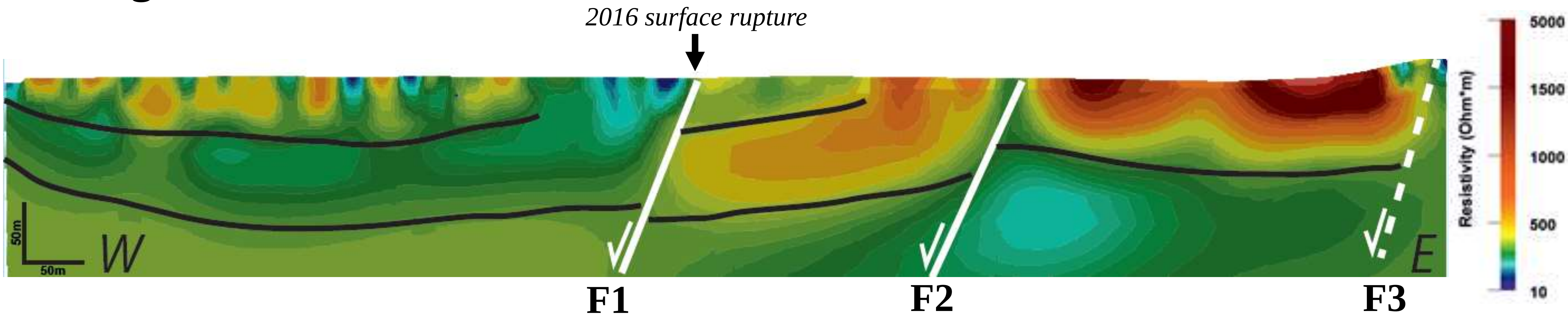

Recovered resistivity model along the transect highlights the presence of two fault splays (solid white lines) belonging to the VBFS and distributed in a > 1 km-wide deformation zone. The westernmost splay is clearly located in correspondence of the surface rupture and it is characterized by a high-angle geometry with a total throw > 50 m . The dip slip dislocation is the expression at depth of the fault splay that activated and ruptured the surface during the 30 October 2016 earthquake. Moving eastward, the resistivity model shows an additional fault splay, not reported in previous works and with no surface expression that dislocates the high resistivity cover attributable to coarse-grained slope deposits. The 2D resistivity model hints to the presence of the basin-bounding fault splay in the easternmost side of the transect (dashed white line). This splay is located on the topographic break at the base of the of the long-term cumulative fault scarp of Mt.Vettore - Mt.Redentore and it is imaged by a sharp horizontal resistivity contrast which abruptly interrupted the prosecution of a high resistive body towards East.

The fluvio-lacustrine materials are clearly imaged as a lower resistivity layer located in the footwall of F1 while coarse debris fan deposits as having very high resistive response and corresponding to the top layer in the model and located in the footwall of F2 and of the inferred F3.

3D survey

RESULTS

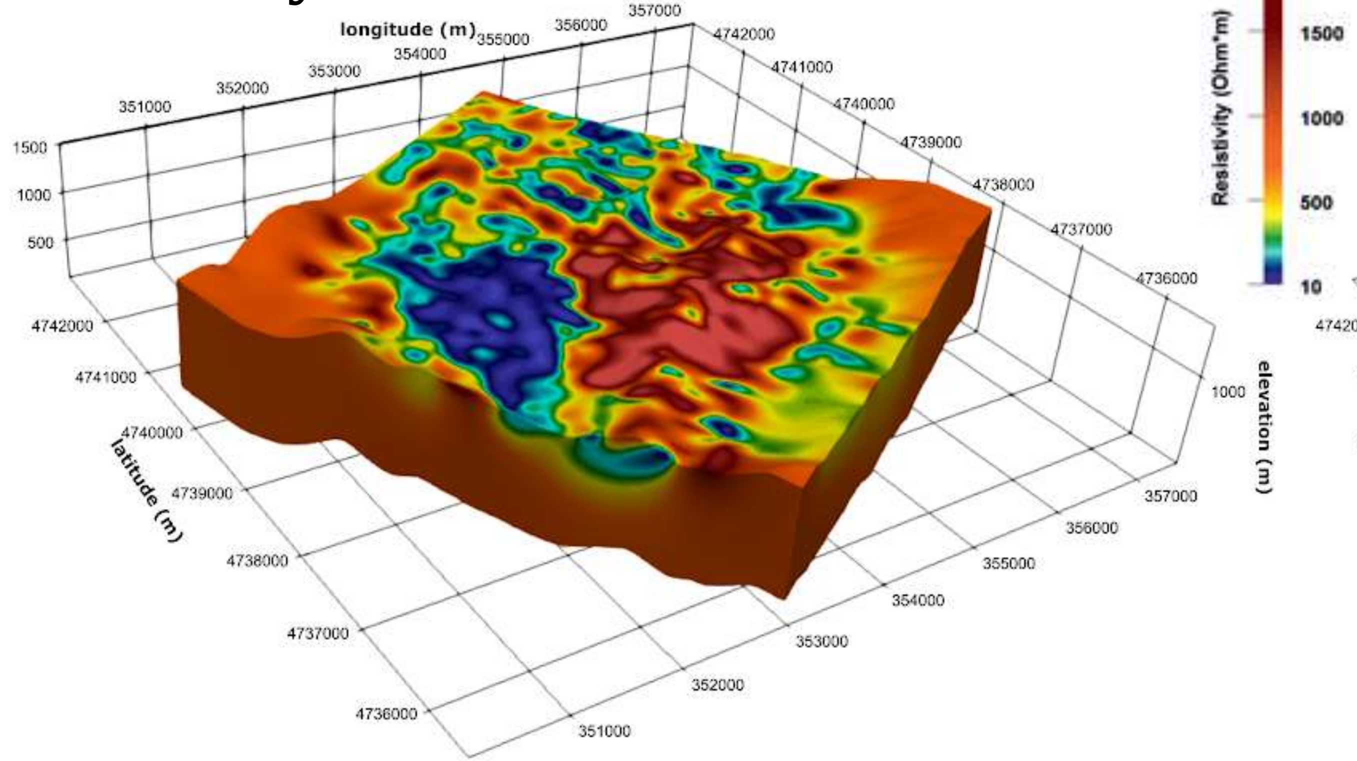

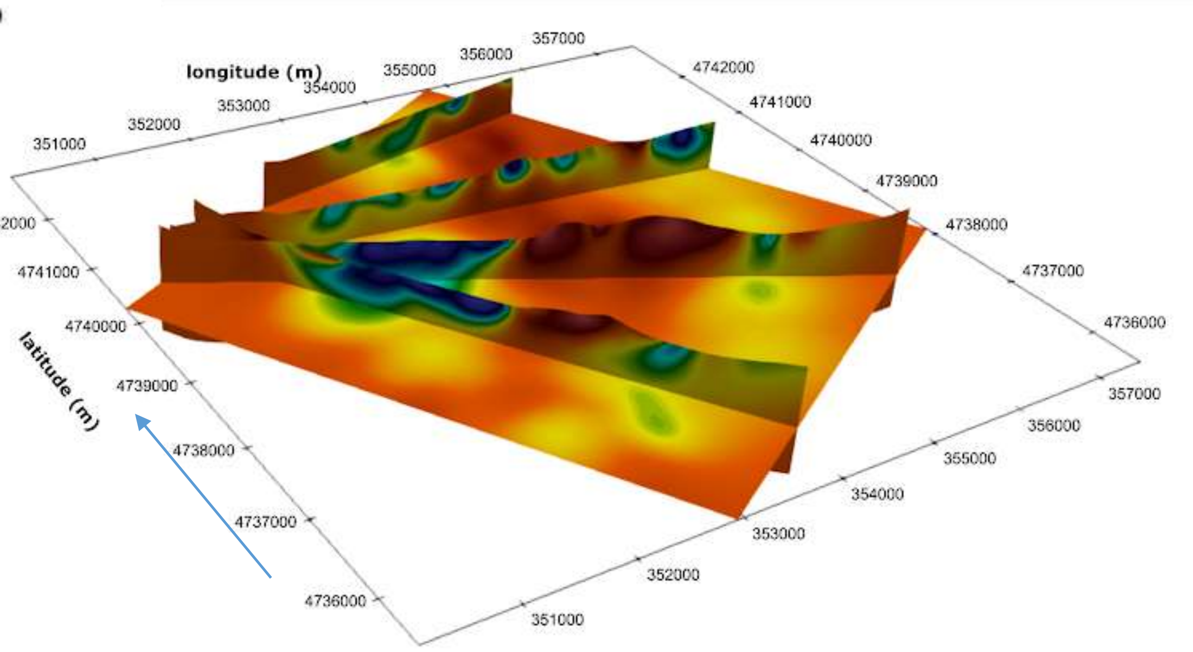

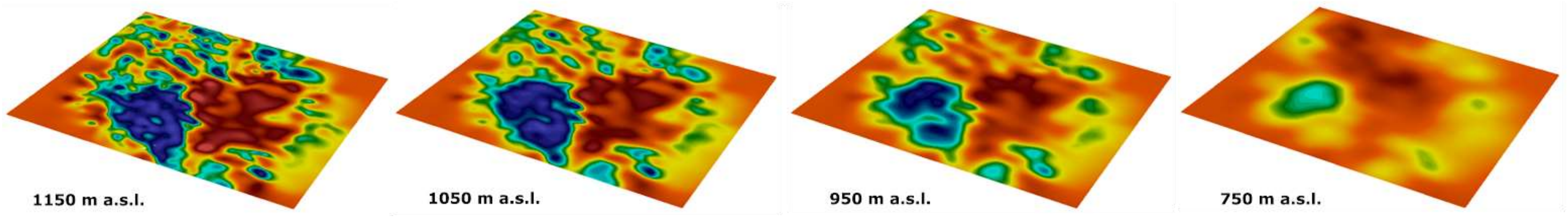

Top left: 3-D Fullwaver resistivity model of the entire survey area. **Top right**: 2-D cross-sections over the horizontal slice at 750 m a.s.l. **Bottom**: slices at different absolute elevations. The wide low-resistive region delineates the deeper portion of the PGC basin infill. Those slices suggest a complex structure with a main depocenter to the south and segmentation to the north, due to the interference of differently oriented fault systems

Two simplified geological cross—sections in the northern (A-A') and the southern part of the basin (B-B') – see left panel for the location of the interpreted sections

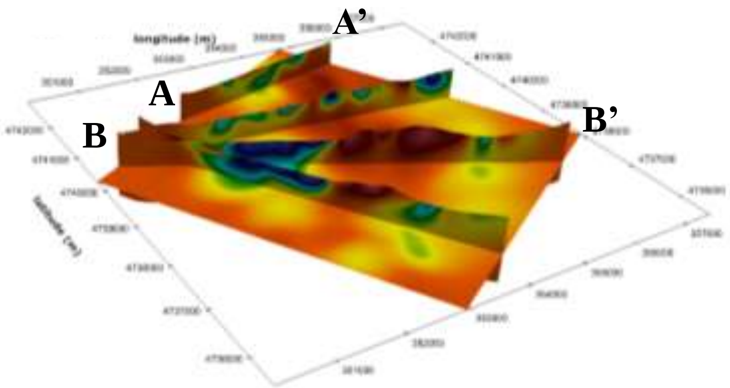

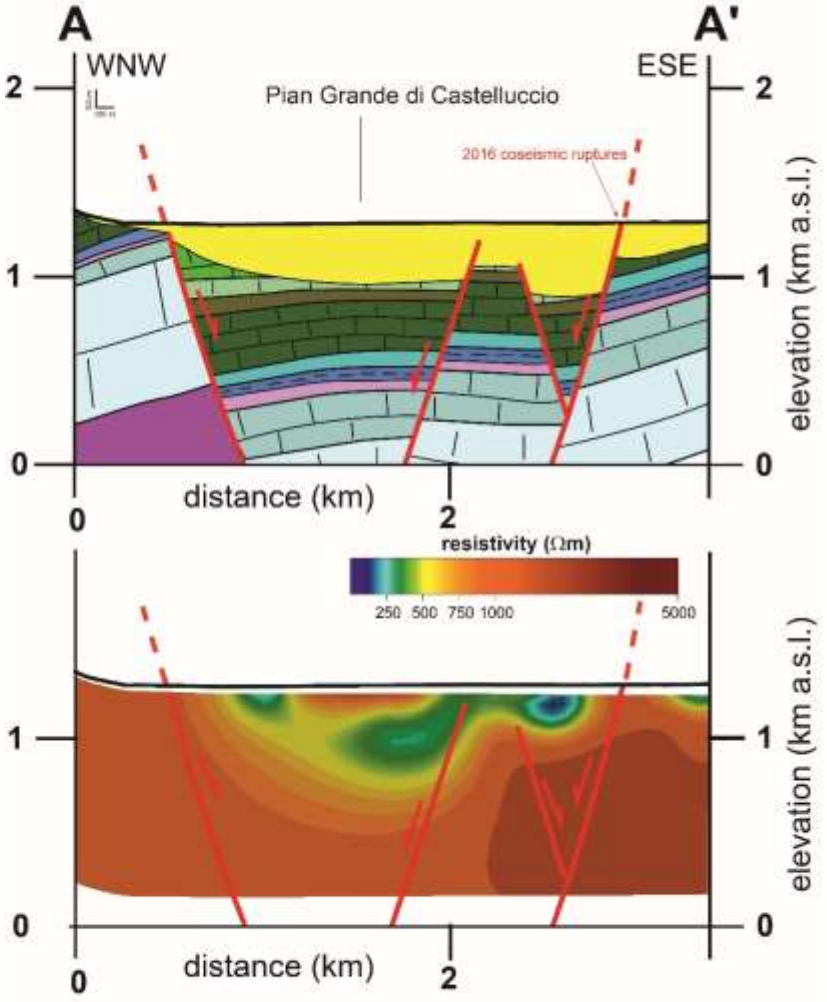

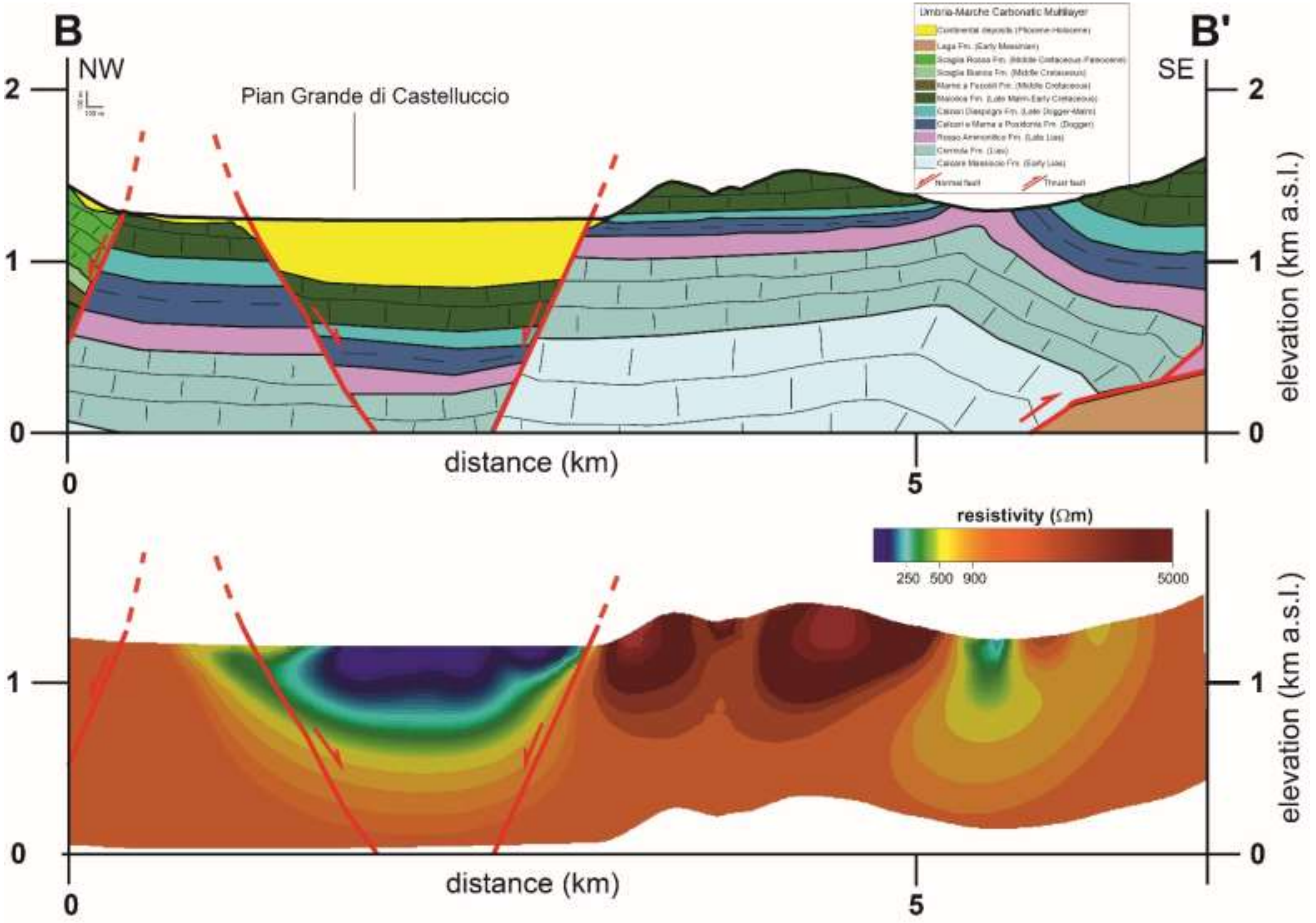

Sketch of **possible deep fault networks** as inferred from the recovered 3D resistivity model (elevation slice at 900 m a.s.l.).

Warning: **very preliminary**, this scheme needs to be checked with other information (i.e. high-resolution seismic profiles already acquired in the area and which data processing are still under review)

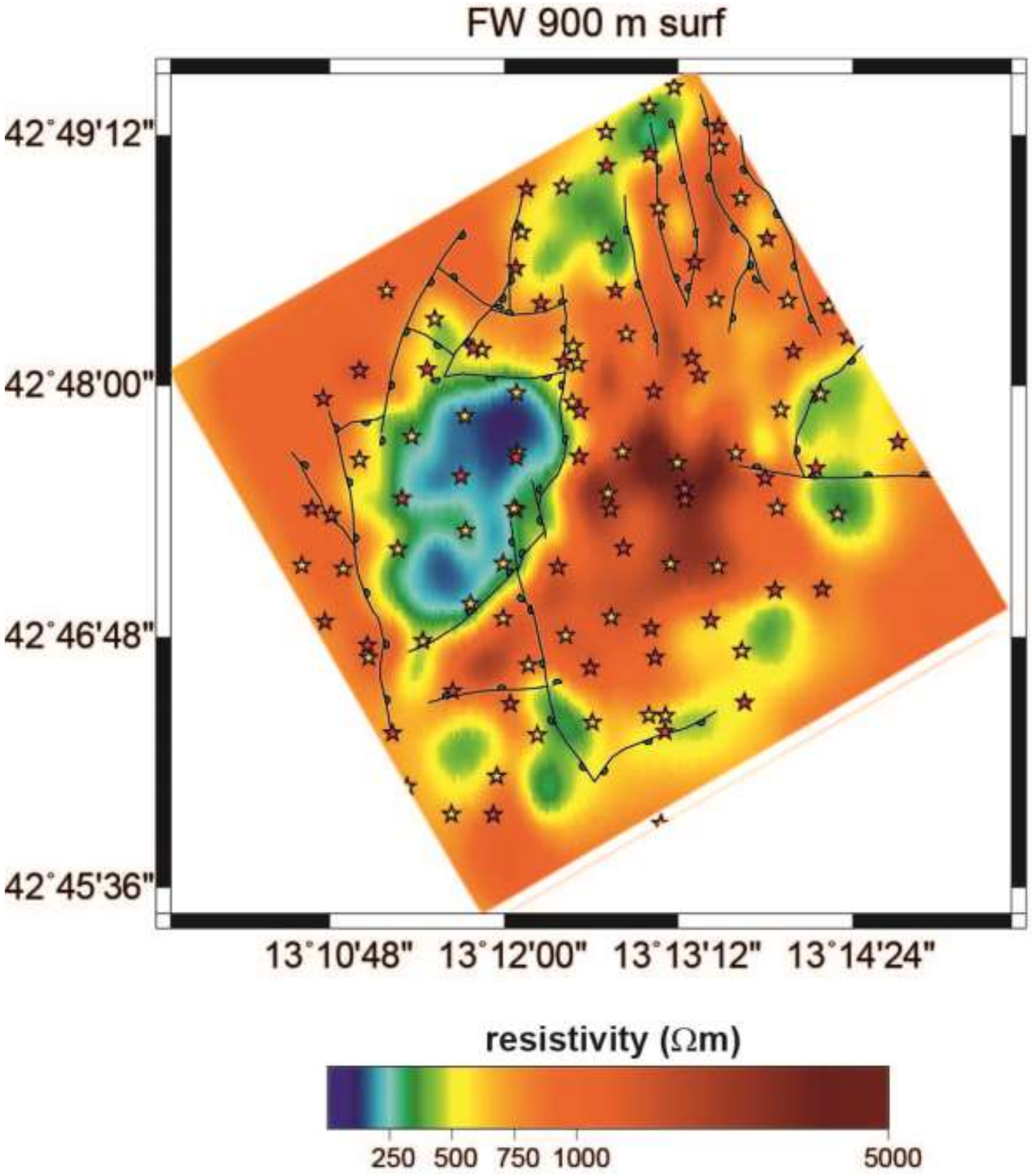

CONCLUSIONS

1 – Large-scale structure of the PGC basin mainly consists of: a) a **main depocenter to the south, > 500 m deep**; b) **complex segmented and shallower basin to the north**.

2 - Main resistivity anomalies trend parallel to the main splays of the VBFS (N150°-170°) in the northern part of the PGC basin while, in the southern part, they appear to parallel the oldest faults system (N20°-30°), **suggesting the interplay of different fault through time**.

3 - Low-resistivity round-shaped anomalies in the Mesozoic substratum to the east of the basin **hints for inherited Miocene compressional structure** as shown in the inset below (sub-parallel to the regional Sibillini thrust).

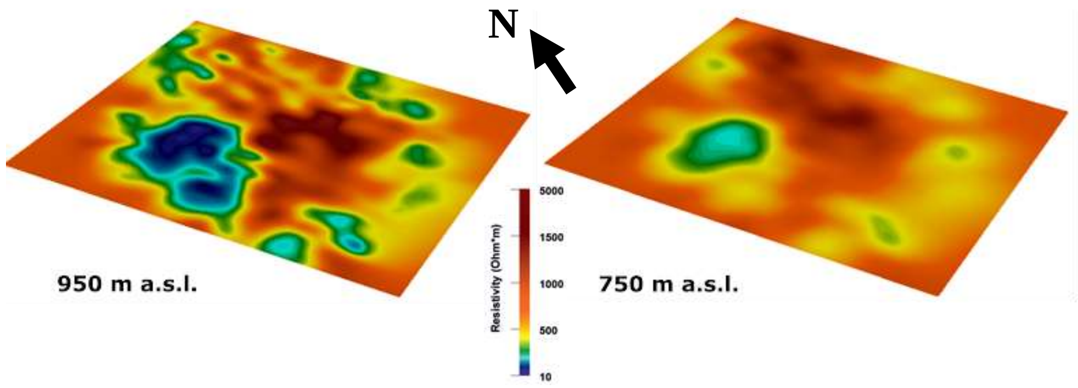

References
Galadini F., Galli P. (2003), Ann. Geophys., 46(5), 815-836, https://doi.org/10.4401/ag-3457.
Villani F., Sapia V. (2017), Tectonophysics, 717(16), 628-644, https://doi.org/10.1016/j.tecto.2017.08.001
Villani et al., (2019), Tectonics, 38, (1), 26-48, https://doi.org/10.1029/2018TC005205
Civico, R., et al., (2018). Journal of Maps, 14(2), 151–160, https://doi.org/10.1080/17445647.2018.1441756

Acknowledgements
This work was funded by Project Top-Down FISR 2016 “L’Italia Centrale in 4D e ricostruzione dei processi geodinamici in atto” TASK 1.2 “Sviluppo di prospezioni geosiche e tecniche di misura innovative ad alta risoluzione per la caratterizzazione del sottosuolo e della deformazione di bacini continentali nell'area epicentrale della sequenza di Amatrice-Visso-Norcia” (Resp: Vincenzo Sapia, Fabio Villani; Chief L. Improta)